J. N. Am. Benthol. Soc., 2002, 21(1):2–15

Water velocity attenuation by stream periphyton and macrophytes in relation to growth form and architecture

WALTER K. DODDS[1] AND BARRY J. F. BIGGS

National Institute of Water and Atmospheric Research Ltd., PO Box 8602, Christchurch, New Zealand

Abstract. Periphyton and macrophytes alter water velocity in streams, influencing movement of solutes and providing microhabitat for other organisms. How assemblages with different growth form and architecture influence water velocity attenuation across mm to dm scales is not well described. A thermistor microprobe was used to measure water velocity through 4 morphologically distinct stream periphyton assemblages and 4 distinct stream macrophyte assemblages in flumes. All assemblages resulted in an exponential decay in velocity with depth. A dense assemblage of diatoms (primarily *Cymbella*) attenuated velocity more than filamentous green algae, filamentous green algae with interspersed diatoms, or a red alga (ANOVA, $p < 0.05$). External water velocity had no significant influence on the coefficient of attenuation in a filamentous green alga (ANOVA, $p = 0.76$). Macrophytes also attenuated water velocity, but attenuation was more variable and, in all cases, attenuation coefficients were less for macrophytes than for periphyton. A model unifying attenuation by periphyton and macrophytes was developed using biomass density (g ash-free dry mass/m^3) as the independent variable and it explained 80% of the variation in attenuation. The relative variance of attenuation coefficients increased sharply as Reynolds number increased above ~500 to 700, suggesting that variance in water velocity was dependent upon the spatial scale of the primary producer through which water is flowing, and that the distinction between periphyton and macrophytes may have real physical ramifications.

Key words: algae, current, flow, hydrodynamics, microphytobenthos, primary producers, submerged plants.

The importance of water velocity as a primary controller of the distribution, composition, and metabolism of photosynthetic organisms in streams is widely recognized (e.g., Biggs 1995, 1996). However, as lotic primary producers establish and grow, they can strongly alter the flow into which they are growing (e.g., Sand-Jensen and Mebus 1996, Nikora et al. 1998a). Such feedback can have a number of important consequences for the ecology of streams, which include delaying downstream transport of dissolved materials (termed 'transient storage zones'; Stream Solute Workshop 1990, DeAngelis et al. 1995); altering sediment deposition regimes (Sand-Jensen 1998, Vermaat et al. 2000) and thus food availability for detritivorous invertebrates; increasing habitat heterogeneity while decreasing shear stress on organisms within the plant mats; influencing epiphyte abundance and community composition (Sand-Jensen et al. 1989, Bergey et al. 1995); and altering nutrient transfer rates to benthic biofilms (Gantzer et al. 1988, Freeman et al. 1995, Borchardt 1996).

Although stream macrophytes reduce velocity near the bed and within the mass of plants, the magnitude of the effect depends greatly upon the growth form and architecture of the plants. For example, Sand-Jensen and Mebus (1996) showed that plants with large leaf areas on bushy shoots reduce water velocity more than plants with streamlined, strap-like leaves. They also documented how the flow resistance of macrophytes led to increased water velocity around the periphery of individual stands of macrophytes, which contributed to the maintenance of a mosaic of patches.

Water velocity is also attenuated by periphyton. Dodds (1991) reported attenuation rates for mats of the filamentous green alga *Cladophora glomerata*, which are even higher than those for macrophytes (e.g., Sand-Jensen and Mebus 1996). However, it is also likely that attenuation rates vary among periphyton communities as a function of their community growth form and architecture, as has been shown for macrophytes.

Macrophyte and periphyton assemblages co-

[1] Present address: Division of Biology, Kansas State University, Manhattan, Kansas 66506 USA. E-mail: wkdodds@ksu.edu

occur in streams. We are aware of no general model that describes the relative attenuation of velocity across the scales at which these different primary producers develop. A model that explicitly considers scale, structure, or assemblage density would be useful because a clear distinction does not always exist between what is considered periphyton and what is considered a macrophyte. For example, *Cladophora* and *Batrachospermum* may be considered small macrophytes or large algal periphyton.

Most general theory on flow through complex canopies comes from the study of airflow through terrestrial vegetation (e.g., Raupach and Thom 1981). These approaches have been applied to the filamentous green alga *Cladophora* in marine environments (Escartín and Aubrey 1995) with some success. However, the relevance of these previous approaches to understanding the effects of different species of periphyton and macrophytes on water velocity in streams across mm to dm scales has not yet been demonstrated. We therefore investigated water velocity through a range of periphyton and macrophyte growth forms and architecture in an attempt to understand factors influencing velocity attenuation by stream primary producers at different scales. We also wished to quantify factors leading to variability in attenuation coefficients (a measure of turbulence and habitat heterogeneity) in these photosynthetic organisms.

Methods

The study was conducted at the NIWA Silverstream Research Facility, 15 km north of Christchurch, New Zealand. Fine-scale thermistor probes (i.e., 1–2 mm resolution) (LaBarbera and Vogel 1976) were used to measure velocity profiles through the periphyton and macrophyte test communities in small and large flumes, respectively.

The thermistor sensors were custom-made and measured total water movement (i.e., they were not sensitive to current direction). The circuitry was connected as in Vogel (1981), and the signal averaged for 5 s with a LI-1000 data logger. The thermistor used for the sensor was a *high-precision* thermistor coated with thermally conductive epoxy, and had a typical response time of 1 s (Betatherm 0.1K1A1–25, Betatherm Corporation, Shrewsbury, Massachusetts). A similar, 3K Ω thermistor was used for the reference that balances the circuit. The sensor was calibrated in a miniflume within which free-stream velocity was measured accurately with a small Ott screw-type current meter. The thermistor was calibrated using water velocities of 3 to 194 cm/s at water temperatures of 15, 20, and 25°C. The calibration was checked again in the miniflume using an Acoustic Doppler Velocimeter (ADV lab version; Sontek/YSI, San Diego, California), with a 3-dimensional probe using the 5-cm working distance. These measurements were made well away from the wall, and calibration curves provided water velocity estimates from the thermistor within 10% of the ADV at water velocities of ~10 cm/s. The probe was mounted on a micromanipulator for accurate positioning.

There was a minor effect of the macrophytes and periphyton on water velocity sensitivity of the thermistor water velocity probes. Artifacts can arise if the sensing thermistor probe comes close to a material with a significantly different thermal conductivity than water (i.e., a rock or a large pocket of air). When thermal conductivity of an interfering material is greater than water, the probe will give a signal >0 when there is no flow. When the interfering material has a thermal conductivity that is less than water, the probe will give a signal <0 when there is no flow. When the probes were placed in periphyton mats or against macrophytes in still water, there was a slight decrease in signal. It was difficult to determine if this occurred because the solid materials have a lower thermal conductivity than the water, or if there are currents induced by thermistor heating of the water that are damped by the solid matrix (i.e., 0 water velocity in the open water is not really 0 water velocity because the heated probe itself generates water movement). Regardless, the potential error in estimated water velocity caused by contact with the producers was <0.5 cm/s in still water.

The working area of the recirculating miniflume used for the periphyton measurements was 15 cm wide × 20 cm long × 15 cm deep. The working section of this flume had parallel flow lines (determined with dye injections), indicating that the vertical and horizontal vectors of velocity were low relative to the longitudinal vector (Dodds and Brock 1998). The coefficient of variation (CV), in water velocity across the

TABLE 1. Characteristics of periphyton assemblages used to assess water velocity attenuation. See Methods for descriptions of assemblage architecture. Dimensions were mapped at measurement velocity (in assemblage 1, at 15 cm/s). Chl = chlorophyll, AFDM = ash-free dry mass. – = not measured.

Periphyton assemblage number and abundant species	Chl *a* (mg/m^2)	Chl *a* (mg/cm^3)	Mass density (g $AFDM/m^3$)
1–Dominant: *Ulothrix*	225	0.015	4250
2a–Dominant: *Ulothrix, Snynedra ulna*; common: *Fragilaria*	341	0.023	2161
2b–Dominant: *Ulothrix*; common: *Synedra ulna*	362	0.036	2475
3–Dominant: *Cymbella kappi, Synedra ulna*; common: unicellular cyanobacterium, *Phormidium, Ulothrix*	1203	0.241	21,714
4–Dominant: *Batrachospermum*; common: *Ulothrix, Synedra ulna*	430	0.043	7692

working section was <4%. Additional measurements in the working section using the ADV flow meter demonstrated that vertical and horizontal velocity was <10% of downstream velocity at 10 cm/s in the working section. The miniflume had an external motor to drive a large propeller for water recirculation, so water heating was <1°C during the course of each measurement. Water velocity profiles without added periphyton, construction details, and water velocity variance in the flume are documented by Dodds and Brock (1998).

The large flume used for macrophyte measurements was 10 m long and 0.75 m wide; the depth and velocity of the water could be controlled from 0 to 0.35 m and 0 to 2.5 m/s, respectively, using different pump settings and slopes (Nikora et al. 1998b). We set the flume at a slope of 0.03%, with the velocity being controlled by discharge (10–170 L/s within a range of 1.5%) and an end gate at the outflow for fine-scale adjustment of backwater. Macrophytes were placed in the central region (between the channel edges) in the area from 5 to 9 m from the leading edge of the flume where parallel flow lines are fully developed (Nikora et al. 1998b). Water was taken directly from the spring-fed Kaiapoi River at 12°C for all macrophyte experiments and discharged back into the stream at the end of the flume. Temperature varied <1°C during each set of measurements.

Measurements were carried out on periphyton and macrophyte patches freshly collected from the Kaiapoi River adjacent to the field station. The materials represented the widest possible range of distinctive assemblage types, from gelatinous microbial mats to large-leaved macrophytes. The filamentous algal masses were held in the miniflume with a small spring-loaded clip at their upstream edges, except for the diatom mat, which was an intact 3 × 7 cm rectangular piece that was held in place with a series of very small pebbles placed around its periphery. Macrophytes were collected from nearly unispecific stands in the river, and each handful was attached to a flat concrete weight on the bed of the flume with wire at the roots. The stalks left the concrete weight at the approximate angle relative to water direction and streambed as occurred naturally where they were collected. Algal and macrophyte masses were mapped (shape, area, and thickness along the length), and water velocity profiles then were determined as described below.

Five periphyton assemblages were used for the analysis (Table 1). The 1st assemblage (1) was a mat of the green alga *Ulothrix zonata*. This mat was almost a single species, with few epiphytes attached to the filaments. It had the simplest architecture, with very flexible filaments forming parallel masses that had an open weave (interfilament gaps of ~0–10 mm depending on the point of sway), no branching, and no secretions of mucilage within or at the base of the mat. The 2nd assemblage (2a) was a more complex, mixed diatom–*Ulothrix zonata* mat. Masses of unbranched *Ulothrix* filaments lying parallel in the flow and intermingled cells of *Synedra* dominated the upper canopy of the mat, but the lower canopy had mucilage and moderate densities of diatoms forming a complex, 3-dimensional array of projections. Thus, the mat had a higher density and smaller interfilament gaps than the monospecific *Ulothrix* mat. The 3rd assemblage (2b) was similar to 2a, but had less diatom material associated with the mat than

TABLE 1. Extended.

Max. depth (cm)	Max. length (cm)	Width at distance from leading edge (cm)			
		0.5	2.0	4.0	6.0
2.0	8	3.0	4.7	4.9	2.7
2.0	7.1	1.0	1.7	2.2	2.7
1.5	15	0.7	1.0	1.1	1.7
0.6	7	3	3	3	3
1.0	2.3	1	2.2	—	—

assemblage 2a, but considerably more than assemblage 1. Assemblage 3 was a tightly attached mucilaginous diatom mat. It formed a cohesive matrix on the substrate with low flexibility. This mat was cut in a single 7 × 3 cm rectangle from the surrounding mat in the streambed to fit in the center of the working section of the miniflume. The final sample (assemblage 4) was a very complex, branched, filamentous mass formed by the red alga *Batrachospermum*. The filaments formed miniature, *tree-like* structures with a relatively long stiff primary filament, and secondary and tertiary branching in the upper canopy. Whorls of small filaments arose from the primary, secondary, and tertiary filaments and formed a dense canopy.

Four replicate velocity profiles were measured in the pure *Ulothrix* mass (assemblage 1) at each of 3 water velocities, whereas velocity profiles were taken at only 1 water velocity rate in assemblages 2a, 2b, and 3 (4 replicates each) and in the *Batrachospermum* (2 replicates). Profiles were taken at 0.5, 2, 4, and 6 cm from the leading edge of assemblages 1, 2a, 2b, and 3 and at 0.5 and 2 cm in the shorter mass of *Batrachospermum*. All periphyton velocity measurements were conducted within 30 min of collection, temperature was read at the beginning and end of the measurement, and the calibration curve appropriate for the measurement was used. Assemblage 1 was measured at 14.5 to 15.5°C, and 2a, 2b, 3, and 4 at 13 to 15°C.

Four macrophytes that varied in architecture were used for analysis of velocity attenuation by large plants (Table 2). Four velocity profiles were measured in the center of 4 separate clumps of each macrophyte type at each of 2 distinct freestream velocities. Profiles were measured within 2 h of collection, and macrophytes were stored in containers placed in the river between collection and measurement.

Following measurement of velocity profiles, periphyton and macrophyte samples were frozen for later analysis. A separate sample of algae was stored in the dark at 3°C and analyzed for assemblage composition with light microscopy within 2 d. Areal biomass and biomass density (biomass per volume of flow occupied) were determined from ash-free dry mass (AFDM) for both producer types. Macrophyte samples were weighed damp, dried at 105°C for 24 h, and reweighed. A subsample was then analyzed for AFDM by ashing for 4 h at 400°C. Chlorophyll *a* was also determined for the periphyton. For AFDM and chlorophyll analyses, each periphyton sample was thawed and homogenized using a blender (Biggs 1987). The sample was then transferred to a narrow-necked bottle, brought to a known volume with water, and shaken thoroughly to obtain a suspension from which 2 separate subsamples were withdrawn. These subsamples were filtered to concentrate the periphyton on separate Whatman GFC-filters for AFDM determination (as determined for macrophytes) and for chlorophyll *a* analysis. For the chlorophyll analysis, boiling 90% ethanol was used as an extractant, absorbance was read on a spectrophotometer, and a correction for phaeopigments was applied following acidification. An extinction coefficient for chlorophyll *a* of 28.66/cm was used (Sartory and Grobbelaar 1984).

Reynolds number (Re) was estimated for each assemblage using water velocity and estimated characteristic lengths. The typical spaces be-

TABLE 2. Characteristics of macrophytes used to assess velocity attenuation. AFDM = ash-free dry mass.

Macrophyte assemblage number and dominant species	Morphology	AFDM		Average of maximum dimensions of 4 clumps used for measurements (cm)		
		(g/m^2)	(g/m^3)	Length	Width	Depth
1–*Myriophyllum triphyllum*	Complex architecture; whorls of small needle-like leaves, and stiff, unbranched stems	96	621	42	21	19
2–*Glyceria fluitans*	Simple; strap-like leaves on long, branched stems	187	1780	57	18	11
3–*Potamogeton crispus*	Moderately complex; long, thin stems, with long, branched stems and tightly packed, linear ovate, crenulate leaves near the end of the stems	183	1339	92	16	14
4–*Elodea canadensis*	Complex; whorls of recurved linear-elliptical leaves and stiff, unbranched stems forming snake-like streamers	134	1020	33	20	14

tween algal filaments or cells are much smaller than those between leaves of macrophytes, so the Re is lower. Characteristic lengths (widths of leaves) that were used to calculate Re for the macrophytes were 100, 50, 10, and 4 mm for *Myriophyllum*, *Glyceria*, *Potamogeton*, and *Elodea*, respectively. Characteristic lengths for periphyton were 0.05, 0.1, 0.01, and 1 mm for assemblages 1 (*Ulothrix*), 2a (*Ulothrix* and *Synedra*, moderate diatom cover), 2b (*Ulothrix* with low diatom cover), 3 (dense diatom mat), and 4 (*Batrachospermum*), respectively. These characteristic lengths are rough estimates based on the average width of the dominant species in each assemblage. It is difficult to determine the characteristic length for complex, unevenly shaped objects (Vogel 1994). However, the characteristic lengths vary by ~4 orders of magnitude, so precise numbers are not necessary for this calculation.

Results

Velocity attenuation in periphyton mats

An exponential curve provided the best fit for the reduction of water velocity with depth in periphyton. This model had the general form:

$$U_z = U_{z-d}\, e^{-vz} \qquad [1]$$

where U_z = water velocity at depth increment z, U_{z-d} = velocity at the previous depth increment z–d, and v is the water velocity attenuation coefficient. Attenuation coefficients were calculated for each depth using the water velocity value at the depth of measurement and the value from the depth immediately above in the same profile. Mean coefficients ranged about threefold among the 4 periphyton assemblages (Table 3).

Values of v were not affected by instream velocity. Similar gradients in velocity were observed in a single *Ulothrix* mass (ANOVA, $p = 0.76$) despite an approximately sevenfold increase in free-stream velocity (Fig. 1). Furthermore, values of v were not significantly different among any of the 3 *Ulothrix* assemblages (assemblages 1, 2a, and 2b; Table 3), nor were they a function of depth (across a substantial decay in absolute velocity) within profiles (ANOVA, $p > 0.10$). This result indicated that v was independent of free-stream velocity, and justified reporting a single value of v for an assemblage based on multiple water velocity profiles taken at a variety of depths.

Once it was verified that v did not vary significantly with depth, regression of natural log-transformed velocity data against depth allowed us to test the ability of a logarithmic model to predict velocity gradients within periphyton assemblages. The variance explained using re-

TABLE 3. Velocity at surface, mean rates of attenuation (v) across all measurements, and range of variance explained by the exponential model for periphyton assemblages. Range of r^2 from regression applied to 4 profiles on all except *Batrachospermum*, which was only large enough for 2 profiles. See Methods for assemblage description, and equation 1 for method to calculate the velocity attenuation coefficient. SE in parentheses.

Assemblage number	Velocity at surface (cm/s)	v(/mm)	Number of attenuation coefficients	Number of profiles	r^2 (range)
1–*Ulothrix*	16 (9)	0.29 (0.04)	24	4	0.94–0.98
1–*Ulothrix*	51 (22)	0.33 (0.05)	24	4	0.83–0.98
1–*Ulothrix*	107 (25)	0.32 (0.05)	24	4	0.82–0.98
2a–*Ulothrix/Synedra*	13 (3)	0.50 (0.14)	20	4	0.79–0.98
2b–*Ulothrix*	6 (2)	0.39 (0.07)	20	4	0.86–0.95
3–*Cymbella/Synedra*	21 (11)	0.96 (0.10)	12	4	0.95–0.99
4–*Batrachospermum*	30 (3)	0.54 (0.16)	10	2	0.52–0.95

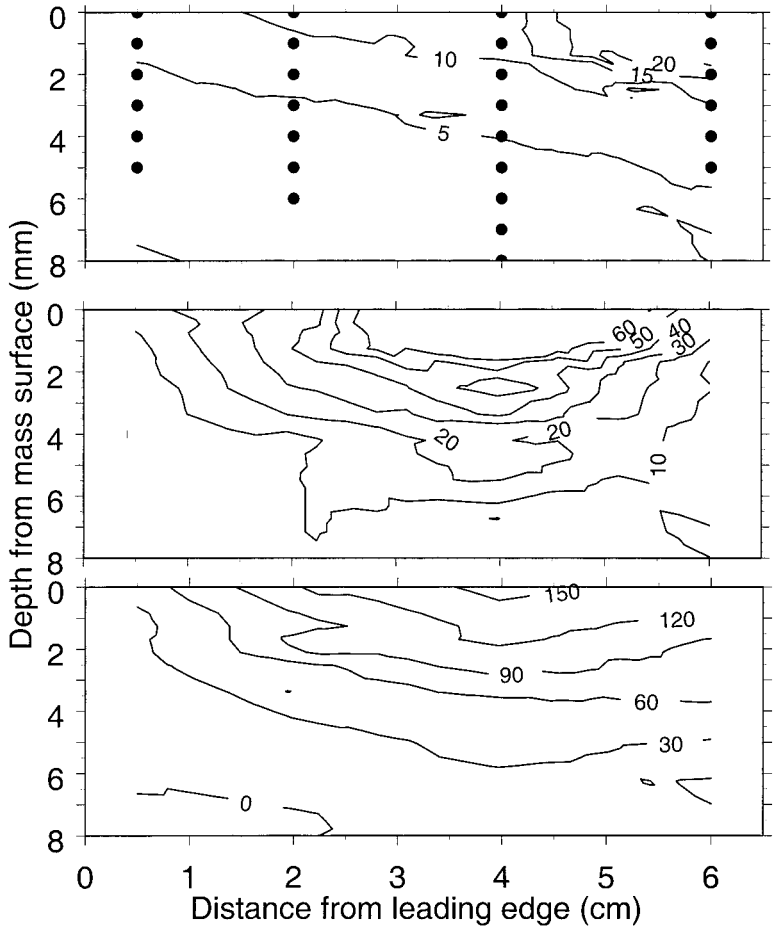

FIG. 1. Water velocity contours in a *Ulothrix* mass (assemblage, Table 1) at 3 levels of external water velocity (15, 38, and 111 cm/s, top graph to bottom, respectively). The measurement points are shown as dots in the top panel. The last depth of measurement at each distance from the leading edge is at the bottom of the filamentous mass. Contours were drawn by Axum (MathSoft, Cambridge, Massachusetts).

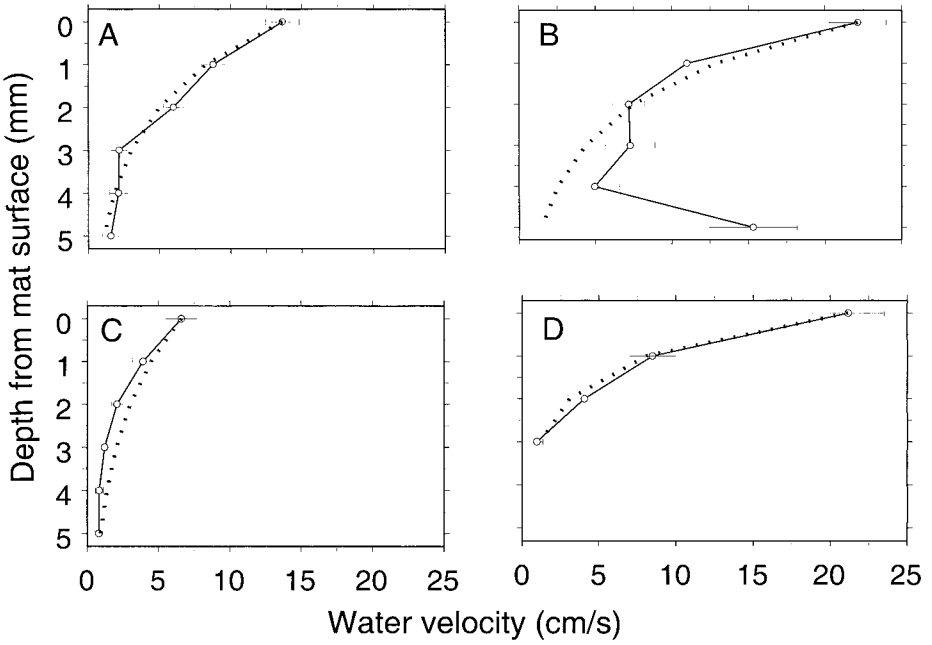

FIG. 2. Relationships between water velocity and depth for 4 periphyton assemblages (Table 1): 2a (A), 4 (B), 2b (C), and 3 (D). Broken line is the exponential model fit to all data. Error bars = ±1 SE.

gression to fit the log-transformed data from each individual profile in each periphyton assemblage generally exceeded 85%, except in *Batrachospermum* for which v was more variable (Table 3).

Analysis of all the periphyton assemblages (i.e., data in Figs 1 and 2) showed a significant effect of assemblage type (and thus growth form and architecture) on v. A consistent decay in velocity occurred with depth into the mat for the filamentous *Ulothrix*-dominated mats (Fig. 2A, C) and the mucilaginous diatom mat (Fig. 2D). The decay was very rapid for the diatoms. Although velocity decreased with depth in the *Batrachospermum* mat down to 4 mm (Fig. 2B), velocity increased again with greater depth, potentially indicating underflow along the base of the mat.

Velocity attenuation coefficients differed significantly between the diatom assemblage and all other periphyton assemblages (Sheffé's method, $p < 0.019$ for all pairwise comparisons of other periphyton types with the diatom mat assemblage). The greater v in the diatom assemblage corresponded to a greater mass density (Table 1). Linear regression revealed a significant positive relationship between v and mass density ($p < 0.0002$). However, this relationship was strongly driven by the diatom assemblage, and was not significant without it.

Velocity attenuation in macrophytes

Water velocity attenuation was much more variable within macrophytes than periphyton (Fig. 3). Analysis of data for the first 9 cm of depth for *Myriophyllum*, *Glyceria*, and *Potamogeton* by species, depth, and external velocity (3-way ANOVA) showed generally lower water velocity in the masses than at the surface (i.e., a significant effect of depth, $p < 0.0000001$). Average velocity in the macrophytes was higher when external velocity was higher (a significant effect of external velocity, $p < 0.05$), but v was not a function of external velocity or depth. Last, the type of macrophyte had a significant effect ($p < 0.000001$) on v (we excluded *Elodea* from this analysis because of highly variable values for v). Pairwise comparison (Sheffe's procedure) revealed that attenuation by *Potamogeton* was significantly greater than that for the other 2 species ($p < 0.001$). An interactive effect of species versus water velocity ($p < 0.0256$) also occurred, supporting the hypothesis that macro-

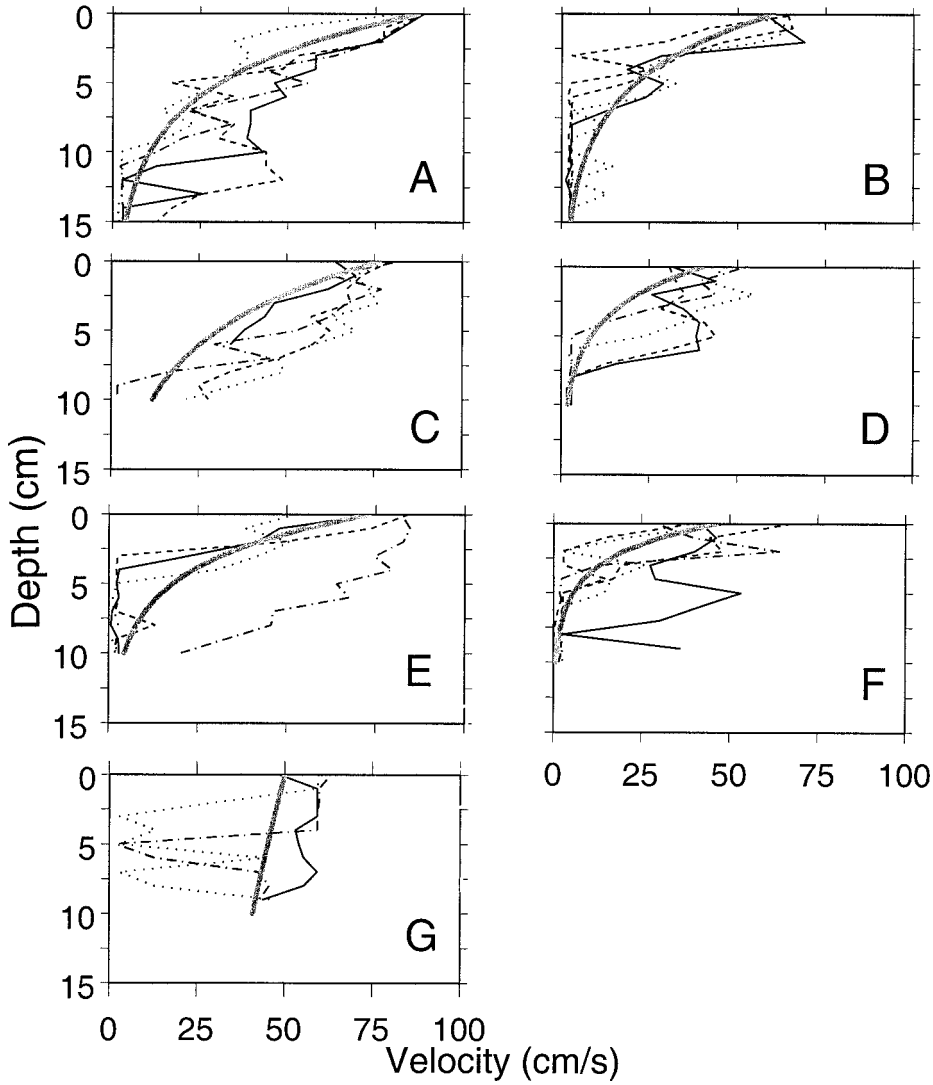

FIG. 3. Relationship between water velocity and depth for 4 profiles taken in 4 separate clumps in each of 4 macrophyte types (Table 2) at various flume mean water velocities: *Myrophyllum*, 20 cm/s (A), *Myriophyllum*, 9 cm/s (B), *Glyceria*, 20 cm/s (C), *Glyceria*, 7 cm/s (D), *Potamogeton*, 18 cm/s (E), *Potamogeton*, 7 cm/s (F), and *Elodea*, 7 cm/s (G). The thin dark lines (solid, dotted, and dashed) represent separate profiles. The thick grey line describes the exponential line fit to data with the attenuation coefficient (v) in Table 4.

phyte architecture influences rates of velocity attenuation.

The velocity at the surface of the macrophytes was often greater than the average velocity in the channels, but this effect was variable. Macrophyte masses tended to compress under higher water velocity, while concurrently forcing flow into the open channel.

Each of the 4 velocity profiles from each macrophyte was fit with linear regression, using untransformed and log-transformed data because v did not vary significantly with depth within an assemblage. Exponential (log-transformed) and linear formulations accounted for similar variance in v among macrophytes (Table 4). Neither model accounted for as much variance as the exponential model with the periphyton mats (Table 3). For comparative purposes, we used

TABLE 4. Mean channel velocity, channel depth, mean (SE) attenuation coefficient (v) for the exponential model, and mean and range of r^2 values (of 4 profiles) for linear- and exponential-decrease models of v within the macrophytes. See Table 2 for description of communities.

Macrophyte assemblage	Avg. channel velocity (m/s)	Water depth (cm)	v (/mm)	Number of attenuation coefficients	Number of profiles	Linear model r^2 (range)	Exponential model r^2 (range)
1–*Myriophyllum triphyllum*	0.09	35	0.021 (0.008)	60	4	0.65 (0.47–0.73)	0.69 (0.53–0.85)
	0.20	21	0.021 (0.011)	60	4	0.79 (0.55–0.91)	0.72 (0.45–0.89)
2–*Glyceria fluitans*	0.07	35	0.031 (0.090)	36	4	0.66 (0.55–0.79)	0.69 (0.61–0.89)
	0.20	22	0.018 (0.060)	36	4	0.87 (0.84–0.90)	0.79 (0.69–0.90)
3–*Potamogeton crispus*	0.07	35	0.042 (0.015)	40	4	0.54 (0.45–0.74)	0.74 (0.54–0.85)
	0.18	18	0.028 (0.014)	40	4	0.71 (0.54–0.88)	0.65 (0.45–0.78)
4–*Elodea canadensis*	0.07	35	0.002 (0.021)	36	4	0.07 (0–0.1)	0.02 (0–0.1)

the exponential model data (i.e., values obtained from equation 1) for both macrophytes and periphyton.

Linking of velocity attenuation in periphyton and macrophytes

We used mass density as a comparative indicator of assemblage form and structure. Using a power-law formulation, we found that this variable explained 81% of the variance in v across all periphyton and macrophyte data, with v being greater when mass density was greater (Fig. 4). This relationship did not hold when macrophytes alone were considered, but it did hold when periphyton alone were considered, mainly because of the very dense diatom mat with high attenuation.

Estimation of the Re for each profile using average water velocity in the profile and average width of the macrophyte or periphyton dominants as the spatial scale showed a weak rela-

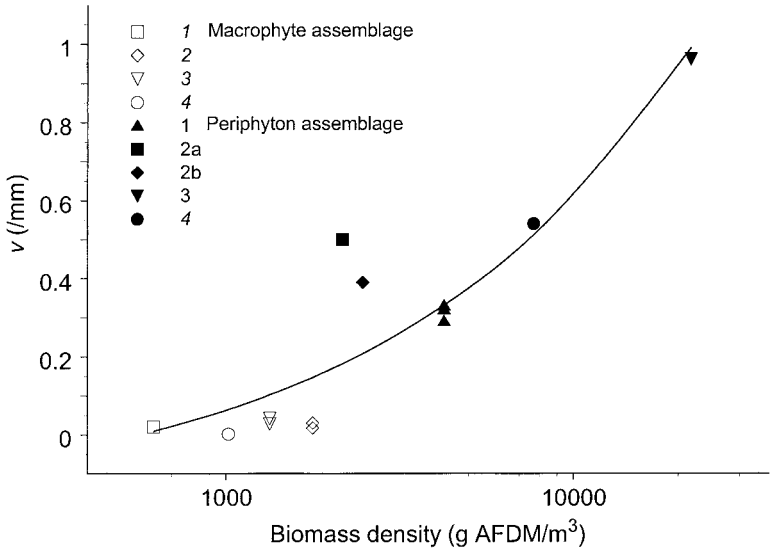

FIG. 4. Relationship between mass density and water velocity attenuation (v) in periphyton and macrophyte mats. Each point represents the v calculated at a specific velocity for each assemblage. The line represents the best-fit curve: v (/mm) = 0.008 × AFDM$^{0.5}$ − 0.190 (g/m^3), adjusted r^2 = 0.81. See Methods and Tables 1 and 2 for assemblage characteristics.

tionship between Re and v for periphyton (Fig. 5A). Water velocity attenuation was generally less variable in the periphyton masses than in the macrophytes (Fig. 5B). The CV increased steadily as Re increased (Fig. 5B). This increase was significant and regular when plotted on a log-log scale, suggesting that variability in v was linked with the degree of turbulence within the producer masses. The CVs in each of the 4 profiles from *Elodea* were high. Both the relationship between v and Re and that between CV of v and RE displayed significant discontinuities (i.e., the distributions were bivariate). A 2-dimensional Kolmogorov–Smirnov test (Garvey et al. 1998) indicated a significant break in the relationship at Re = 606 for v and Re = 713 for CV ($p < 0.002$). Breakpoint regression (a quasi-Newton search method to fit 2 straight lines to the data) was also used to check for a significant breakpoint in the relationships of v and variance with Re. The breakpoint regression indicated discontinuities at Re = 2 for v and Re = 500 for variance. Both models fit substantially better than standard linear regression. This discontinuity possibly coincides with a transition from laminar to turbulent flow within the beds.

Discussion

Limitations of our measurements and modeling approaches

Attenuation of air velocity in plant canopies has been well studied and modeled with at least 3 equations (Raupach and Thom 1981). These equations were used by Escartín and Aubrey (1995) to fit water velocity profiles in marine *Cladophora* mats, but none of them worked well. Our approach of empirically fitting an exponential model to v for our primary producer assemblages enabled us to describe and compare attenuation, but did not provide a specific mechanism to link small changes in architecture (e.g., comparing similar macrophytes, or assessing the effects of variable amounts of diatoms intermingled in filamentous algae) to v.

Our method of measuring water velocity cannot discern direction of flow. Instruments such as acoustic or laser Doppler velocity meters can make small-scale determinations of velocity vectors in all 3 directions, but cannot make measurements within submerged plant masses. Movement of algal thalli or absorption of light or sound by a periphyton or macrophyte mass makes it difficult to use such instruments for measuring velocities within plant masses. This problem has been circumvented previously by placing tubes through algal mats and using a laser Doppler velocity meter (Escartín and Aubrey 1995). Such tubes may influence water velocity, limit the number of points that can be measured, and disturb the structural integrity of plant masses. The thermistor probes we used for velocity measurement at least allowed determination of total v with depth in the assemblages. A similar technique was used by Losee and Wetzel (1993) and Sand-Jensen and Mebus (1996) in macrophytes. In contrast, Madsen and Warncke (1983) used dissolution of salt crystals as a relative measure of total water movement through macrophyte beds.

Potential linkages of attenuation models with material transport

The uptake of nutrients in flowing water is dependent on water velocity (Stevenson 1996, Wheeler 1988). Uptake is often stimulated by increased water velocity (e.g., Stevenson and Glover 1993). The situation is relatively simple in very cohesive algal assemblages where no flow occurs and transport depends mainly upon molecular diffusion and the thickness of the diffusion boundary layer surrounding the assemblage (Sylvester and Sleigh 1985). However, as shown in our study (and others), some filamentous algal assemblages have measurable water velocity through the biomass (Dodds 1991, Dodds and Gudder 1992, Escartín and Aubrey 1995), which has substantial influence on movement of dissolved material through the algal mass (Mulholland et al. 1994, Escartín and Aubrey 1995). We demonstrated that v in submerged patches of primary producers is highly variable depending on architecture. Variation in water velocity will lead to corresponding variation in advective transport of dissolved nutrients. Thus, rates of supply of essential minerals, which then could limit algal and macrophyte production, will also be variable. Our results suggest that such effects of primary producer architecture on flow-through rates would be greatest at low free-stream velocities and within denser, more cohesive mats that have greater v (e.g., periphyton assemblages in general and specifically mucilaginous diatom communities).

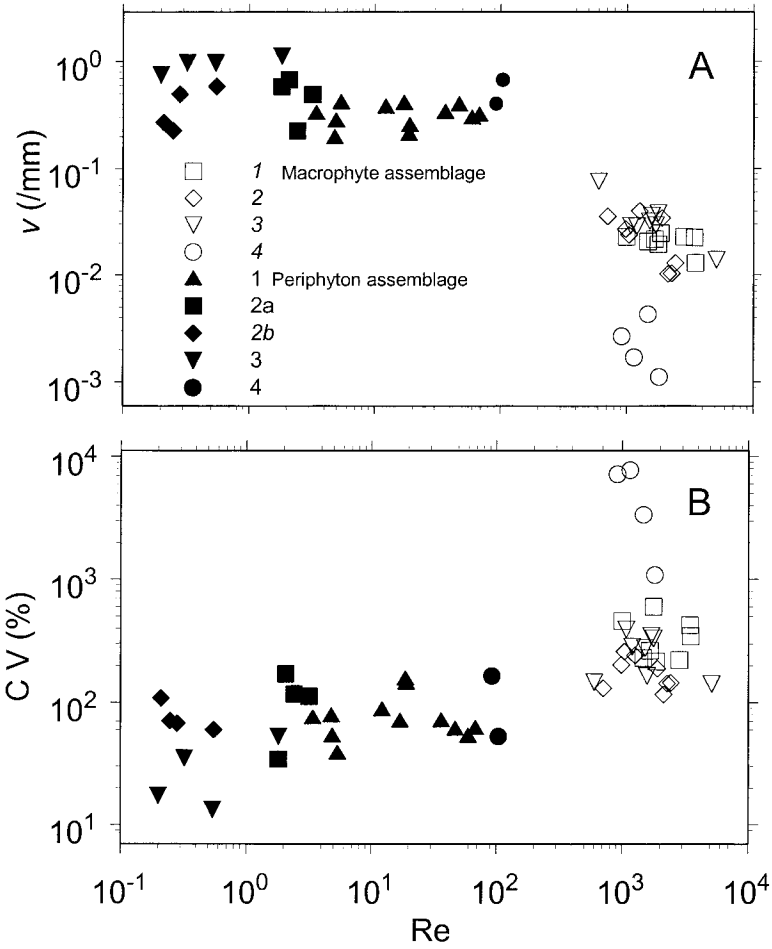

FIG. 5. Relationship between calculated Reynolds number (Re) water velocity attentuation (v) (A) and coefficient of variation (CV) (B) of v calculated for each profile. See Tables 1 and 2 for assemblage characteristics. Regression analysis of data in (B), without *Elodea* data, showed that the relationship was highly significant ($p < 0.0001$, $r^2 = 0.58$).

An exponential model of transport linked to biomass density, mirroring our attenuation model, could assist understanding and comparing relative rates of nutrient delivery among primary producer masses in lotic systems. For example, variable attenuation/mass transfer related to primary producer architecture and growth form may help explain the results of Biggs et al. (1998) who found that open-weave filamentous green algal periphyton, within which v was relatively low, dominated low-velocity habitats in streams. Denser, short, filamentous, and stalked communities, in which moderate v occurred, dominated moderate-velocity habitats, and dense mucilaginous communities, in which v was high, required high-velocity waters for growth.

Inspection of the literature on nutrient uptake in flowing waters provides a confusing picture of the influence of water velocity on nutrient flux and uptake, which may be clarified if future investigators also consider v within periphyton masses. Bothwell (1989) suggested that uptake kinetics governed growth of a diatom mat at PO_4^{3-} concentrations <2 μg/L, but diffusion controlled growth at higher concentrations. Similar patterns were noted by Mulholland et al. (1990) for whole-stream PO_4^{3-} additions; Michaelis-Menten type uptake kinetics predominated below ~2 μg/L PO_4^{3-}, but uptake did not

appear to saturate above that point. This lack of uptake saturation was attributed to abiotic absorption of PO_4^{3-} at higher concentrations. Last, Borchardt et al. (1994) demonstrated biphasic uptake of PO_4^{3-} by a filamentous green algal species (*Spirogyra fluviatilis*). All 3 factors (transport limitation, abiotic uptake, and biphasic uptake) could have influenced the results of Bothwell (1989) and Mulholland et al. (1990). More detailed consideration of v within mats may help explain these prior results. For example, the thick diatom mats used by Bothwell (1989) would be expected to be strongly transport-limited based on our attenuation model, and would thus be expected to be limited by diffusion rate of nutrients, as shown in his experiments.

Scale, architecture, turbulence, and v

Flow through a macrophyte mass is clearly more complex than through periphyton. Large macrophyte beds may have a wide range of velocities within the canopy (our results, also Sand-Jensen 1997, 1998). However, despite variation in v, most macrophytes in streams will have regions of reduced water velocity. These regions will affect solute transport as described above for periphyton. Perhaps more important for macrophytes, though, is that these areas of reduced velocity can serve as flow refugia for invertebrates (e.g., Suren 1991). Our measurements and attenuation calculations suggest that velocities can be reduced sufficiently in high-gradient streams to permit the existence of many *slow-water* taxa such as oligochaetes and some mollusks where normally only *fast-water* taxa would exist. Thus, macrophytes have the potential to increase reach-scale biodiversity through increasing habitat heterogeneity (Suren 1991).

Scale is clearly important in the magnitude and variation of v among aquatic primary producers. At spatial scales <1 mm and with biologically realistic water velocities, Re values predict laminar flow, but at scales >1 mm, they predict turbulent flow (Vogel 1994). Thus, we calculated Re for each individual profile and related it to the mean value of v and the variation of v within that profile. Our data were consistent with a transition from laminar to turbulent flow at $Re > 2$. The 2 statistical techniques used gave somewhat variable numbers, which indicated that the transition between turbulent and laminar flow is not sharply defined. As Vogel (1994) said, ''Most biologists who have heard of the boundary layer have the fuzzy notion that it's a distinct region rather than the distinct notion that it's a fuzzy region''.

Our data suggest that an exponential model of v is superior to a linear model for periphyton assemblages. We can define periphyton assemblages as having $Re < 500$ to 700 (except see Sand-Jensen and Pedersen 1999). In these assemblages, values of v are expected to range from 0.3 to 1.0/mm, with the greatest values of v found in dense, cohesive, mucilaginous algal mats. Macrophytes (with $Re > 500$–700) can be characterized by linear or exponential v and high water velocity variance. Exponential v values in this study ranged from 0.02 to 0.04/mm. However, at the dm scale, v was highly variable and CVs for v often exceeded 100%.

Although the factors that specifically control variation in v likely relate to the architecture and growth form of the producer communities, there is no single variable that directly quantifies the range of these features adequately among benthic primary producer communities in streams. However, we found that mass density provided an adequate surrogate variable for these features in our study communities. Using this variable, it was possible to develop a model to unify the effects of different community types on v along a continuum from macrophytes with loosely aggregated, simple, strap-like leaves such as *Glyceria* to nonfilamentous, mucilaginous, diatom mats composed of *Cymbella*. With further development and calibration, such a model could prove very useful for predicting and understanding variations in downstream solute transport, fine-sediment deposition (including particulate organic matter), habitat heterogeneity (including the development and potential use of refugial habitat by stream invertebrates and fish), and rates of nutrient mass transfer to benthic primary producers.

Acknowledgements

We thank D. Gudder and A. Stokes for technical assistance, and Patricia Chambers and anonymous reviewers for their helpful comments. This is contribution no. 00384J from the Kansas Agricultural Experiment Station. The United States Natural Science Foundation, International Programs, and Konza LTER supported

the research. Support was also received through the New Zealand Foundation for Research, Science and Technology program ''Environmental Hydrology and Habitat Hydraulics'' (Contracts CO1519 and CO1813).

Literature Cited

BERGEY, E. A., C. A. BOETTIGER, AND V. H. RESH. 1995. Effects of water velocity on the architecture and epiphytes of *Cladophora* (Chlorophyta). Journal of Phycology 31:264–271.

BIGGS, B. J. F. 1987. The effects of sample storage and mechanical blending on the quantitative analysis of river periphyton. Freshwater Biology 18:197–203.

BIGGS, B. J. F. 1995. The contribution of flood disturbance, catchment geology and land use to the habitat template of periphyton in stream ecosystems. Freshwater Biology 33:419–438.

BIGGS, B. J. F. 1996. Hydraulic habitat of plants in streams. Regulated Rivers: Research and Management 12:131–144.

BIGGS, B. J. F., D. G. GORING, AND V. I. NIKORA. 1998. Subsidy and stress responses of stream periphyton to gradients in water velocity as a function of community growth form. Journal of Phycology 34:598–607.

BORCHARDT, M. A. 1996. Nutrients. Pages 183–227 *in* R. J. Stevenson, M. L. Bothwell, and R. L. Lowe (editors). Algal ecology: freshwater benthic ecosystems. Academic Press, San Diego, California.

BORCHARDT, M. A., J. P. HOFFMANN, AND P. W. COOK. 1994. Phosphorus uptake kinetics of *Spirogyra fluviatilis* (Charophyceae) in flowing waters. Journal of Phycology 30:403–417.

BOTHWELL, M. L. 1989. Phosphorus-limited growth dynamics of lotic periphytic diatom communities: areal biomass and cellular growth rate responses. Canadian Journal of Fisheries and Aquatic Sciences 46:1293–1301.

DEANGELIS, D. L., M. LOREAU, D. NEERGAARD, P. J. MULHOLLAND, AND E. R. MARZOLF. 1995. Modeling nutrient-periphyton dynamics: the importance of transient storage zones. Ecological Modeling 80:149–160.

DODDS, W. K. 1991. Microenvironmental characteristics of filamentous algal communities in flowing freshwaters. Freshwater Biology 25:199–209.

DODDS, W. K., AND J. BROCK. 1998. A portable flow chamber for *in situ* determination of benthic metabolism. Freshwater Biology 39:49–59.

DODDS, W. K., AND D. A. GUDDER. 1992. The ecology of *Cladophora*. Journal of Phycology 28:415–427.

ESCARTÍN, J., AND D. G. AUBREY. 1995. Flow structure and dispersion within algal mats. Estuarine Coastal and Shelf Science 40:451–472.

FREEMAN, C. P., J. CHAPMAN, K. GILMAN, M. A. LOCK, B. REYNOLDS, AND H. S. WHEATER. 1995. Ion exchange mechanisms and the entrapment of nutrients by river biofilms. Hydrobiologia 297:61–65.

GANTZER, C. J., B. E. RITTMANN, AND E. E. HERRICKS. 1988. Mass transport to streambed biofilms. Water Research 22:709–722.

GARVEY, J. E., E. A. MARSCHALL, AND R. A. WRIGHT. 1998. From star charts to stoneflies: detecting relationships in continuous bivariate data. Ecology 79:442–447.

LABARBERA, M., AND S. VOGEL. 1976. An inexpensive thermistor flow meter for aquatic biology. Limnology and Oceanography 21:750–756.

LOSEE, R. F., AND R. G. WETZEL. 1993. Littoral flow rates within and around submersed macrophyte communities. Freshwater Biology 29:7–17.

MADSEN, T. V., AND E. WARNCKE. 1983. Velocities of currents around and within submerged aquatic vegetation. Archiv für Hydrobiologie 97:389–394.

MULHOLLAND, P. J., A. D. STEINMAN, AND J. W. ELWOOD. 1990. Measurement of phosphorus uptake length in streams: comparison of radiotracer and stable PO_4 releases. Canadian Journal of Fisheries and Aquatic Sciences 47:2351–2357.

MULHOLLAND, P. J., A. D. STEINMAN, E. R. MARZOLF, D. R. HART, AND D. L. DEANGELIS. 1994. Effect of periphyton biomass on hydraulic characteristics and nutrient cycling in streams. Oecologia (Berlin) 98:40–47.

NIKORA, V. I., D. G. GORING, AND B. J. F. BIGGS. 1998a. A simple model of stream periphyton-flow interactions. Oikos 81:607–611.

NIKORA, V. I., D. G. GORING, AND B. J. F. BIGGS. 1998b. Silverstream eco-hydraulics flume: hydraulic design and tests. New Zealand Journal of Marine and Freshwater Research 32:607–620.

RAUPACH, M. R., AND A. S. THOM. 1981. Turbulence in and above plant canopies. Annual Review of Fluid Mechanics 13:97–129.

SAND-JENSEN, K. 1997. Macrophytes as biological engineers in the ecology of Danish streams. Pages 74–100 *in* K. Sand-Jensen and O. Pedersen (editors). Freshwater biology: priorities and development in Danish research. G. E. C. Gad, Copenhagen.

SAND-JENSEN, K. 1998. Influence of submerged macrophytes on sediment composition and near-bed flow in lowland streams. Freshwater Biology 39: 663–679.

SAND-JENSEN, K., D. BORG, AND E. JEPPESEN. 1989. Biomass and oxygen dynamics of the epiphyte community in a Danish lowland stream. Freshwater Biology 22:431–443.

SAND-JENSEN, K., AND J. R. MEBUS. 1996. Fine-scale patterns of water velocity within macrophyte patches in streams. Oikos 76:169–180.

SAND-JENSEN, K., AND O. PEDERSEN. 1999. Velocity gra-

dients and turbulence around macrophyte stands in streams. Freshwater Biology 42:315–328.

SARTORY, D. P., AND J. U. GROBBELAAR. 1984. Extraction of chlorophyll *a* from freshwater phytoplankton for spectrophotometric analysis. Hydrobiologia 114:177–187.

STEVENSON, R. J. 1996. The stimulation and drag of current. Pages 321–340 *in* R. J. Stevenson, M. L. Bothwell, and R. L. Lowe (editors), Algal ecology: freshwater benthic ecosystems. Academic Press, San Diego, California.

STEVENSON, R. J., AND R. GLOVER. 1993. Effects of algal density and current on ion transport through periphyton communities. Limnology and Oceanography 38:1276–1281.

STREAM SOLUTE WORKSHOP. 1990. Concepts and methods for assessing solute dynamics in stream ecosystems. Journal of the North American Benthological Society 9:95–119.

SUREN, A. M. 1991. Bryophytes as invertebrate habitat in two New Zealand alpine rivers. Freshwater Biology 26:399–418.

SYLVESTER, N. R., AND M. A. SLEIGH. 1985. The forces on microorganisms at surfaces in flowing water. Freshwater Biology 15:433–448.

VERMAAT, J. E., L. SANTAMARIA, AND P. J. ROOS. 2000. Water flow across and sediment trapping in submerged macrophyte beds of contrasting growth form. Archiv für Hydrobiologie 148:549–562.

VOGEL, S. 1981. Life in moving fluids. Princeton University Press, Princeton, New Jersey.

VOGEL, S. 1994. Life in moving fluids. 2nd edition. Princeton University Press, Princeton, New Jersey.

WHEELER, W. N. 1988. Algal productivity and hydrodynamics—a synthesis. Progress in Phycological Research 6:23–58.

Received: 5 April 2001
Accepted: 24 September 2001